ELSEVIER

Thermochimica Acta 293 (1997) 93–100

thermochimica acta

Thermochemical effects in the development of mesoporous alumino–phosphoro–vanadates from ammonium nitrate precursors

Konstantina M. Kolonia, Dimitris E. Petrakis, Tiberius C. Vaimakis, Evangelos D. Economou, Philippos J. Pomonis*

Department of Chemistry, University of Ioannina, Ioannina 45110, Greece

Received 20 May 1996; accepted 2 January 1997

Abstract

Mesoporous alumino–phosphoro–vanadate solids were prepared by heating precipitates of the corresponding metals containing ammonium nitrate salts. The materials obtained contained the elements Al : P : V=100 : X : Y, where X, Y=0, 5, 10, 20 (16 samples overall). Thermogravimetric analysis showed that the addition of P or V in the solids influences the endo- and exothermicity of the NH_4NO_3 decomposition, driving the net result from highly endothermal at no addition of P and/or V to almost neutral at high addition (20%) of those heteroatoms. The activation energies, calculated according to the Coats–Redfern procedure, were found to increase on adding 5% of P or V and then to drop at higher addition. The order of the decomposition reaction drops from ≈0.5 to 0 at 20% of P and/or V heteroatoms. The materials obtained had a high surface area (BET) which increases from 200 $m^2 g^{-1}$ for pure alumina to almost 400 $m^2 g^{-1}$ on addition of 5–10% of P and/or V, while further addition of those heteroatoms decreases the surface area to its original values. The maximum of the surface area appears in samples where the NH_4NO_3 decomposition follows almost equal endothermic and exothermic routes. © 1997 Elsevier Science B.V.

Keywords: Mesoporous; Alumino; Phosphoro; Vanadate; Ammonium nitrate

1. Introduction

The development of mesoporous solids with pore radius 10 Å<r_p<250 Å and well defined surface area characteristics is considered a matter of technological priority since such materials can be used as membranes in separation technology, including ultrafiltration, microfiltration and pervaporation applications [1,2]. Recently, Beck et al. succeeded in preparing tailor-made mesoporous silicate/aluminosilicate solids [3,4] employing organic template agents with varying carbon chain. Such materials possess an extremely well-defined porosity but lack any surface acidity since the organic template, which is burned during heating of the precursor material, destroys the Brönsted and Lewis surface acid centres. Nevertheless, such acid centres might be valuable for selective adsorption and surface catalysis.

An alternative method for the preparation of mesoporous solids requires the use of a non-organic material like ammonium nitrate (AN) as a template. This substance is decomposed upon heating towards gases (N_2, H_2O, NH_3, N_2O) which escape from the solid matrix leaving back a more or less well-defined

*Corresponding author. Tel.: 00 30 651; fax: 00 30 651/44836.

PII S0040-6031(97)00069-5

porosity [5]. What is perhaps more important is that such materials possess a surface acidity which in the case of alumino–phosphates [6] is controlled by the amount of P added. Phosphorous at 10–15% addition increases the specific surface area of such solids for reasons which are related to structural and thermodynamic reasons [6]. The purpose of the present work is to investigate the thermochemical characterisation of NH_4NO_3 decomposition on Al–P–V matrices. The final products obtained after heating these precursors at T=600°C are Al–P–V–O solids with high surface area and pore volumes. The vanadium has been included in the study since it is a pentavalent element and like phosphorous is not easily incorporated into alumina. So, it was decided to examine the synergistic affect of those two elements on the thermochemical routes of NH_4NO_3 decomposition as well as the surface area and pore volume characteristics of the final products obtained.

2. Experimental

The specimens used in the experiments (Table 1) contained the elements Al : P : V in ratios 100 : X : Y where X, Y=0, 5, 10, and 20.

Table 1
Composition of samples prepared, their designation, the BET specific surface areas (ssa) and pore volumes (V_p), of the fired (600°C) solids

Sample composition	Designation	ssa ($m^2\ g^{-1}$)	V_p (cc g^{-1})
$Al_{100}P_0V_0$–AN	P_0V_0	201	0.430
$Al_{100}P_0V_5$–AN	P_0V_5	270	0.446
$Al_{100}P_0V_{10}$–AN	P_0V_{10}	302	0.497
$Al_{100}P_0V_{20}$–AN	P_0V_{20}	177	0.456
$Al_{100}P_5V_0$–AN	P_5V_0	245	0.518
$Al_{100}P_5V_5$–AN	P_5V_5	353	0.703
$Al_{100}P_5V_{10}$–AN	P_5V_{10}	359	0.833
$Al_{100}P_5V_{20}$–AN	P_5V_{20}	286	0.743
$Al_{100}P_{10}V_0$–AN	$P_{10}V_0$	320	1.192
$Al_{100}P_{10}V_5$–AN	$P_{10}V_5$	386	1.146
$Al_{100}P_{10}V_{10}$–AN	$P_{10}V_{10}$	322	1.109
$Al_{100}P_{10}V_{20}$–AN	$P_{10}V_{20}$	305	1.020
$Al_{100}P_{20}V_0$–AN	$P_{20}V_0$	239	0.928
$Al_{100}P_{20}V_5$–AN	$P_{20}V_5$	336	0.475
$Al_{100}P_{20}V_{10}$–AN	$P_{20}V_{10}$	258	0.358
$Al_{100}P_{20}V_{20}$–AN	$P_{20}V_{20}$	200	0.245

AN – Ammonium nitrate.

The preparation took place as follows: Calculated amounts of $Al(NO_3)_3{\cdot}6H_2O$ (Merck p.a.) and phosphoric acid (Ferak p.a.) were dissolved in 100 ml of distilled water. Calculated amounts of V_2O_5 (Ferak p.a.) were dissolved in 25 ml of 25% NH_3 (Ferak p.a.) and a colourless solution was obtained. This solution was added in the first one and then ammonia was added in the mixture until the final pH reached a value of 9.5.

The specimens were then carefully dried at 105°C and then fired at 400°C for 4 h, ground and again fired at 600°C for 4 h under atmospheric conditions.

The specific surface areas of the final products, obtained after heating the solids at 600°C for 4 h were determined using the multipoint BET method in a Sorpty 1900 apparatus. The results are included in Table 1.

The thermogravimetric analysis of the unheated solids took place in a Chyo-TRDA-3H thermal balance with simultaneous recording of temperature (T), thermogravimetry (TG), differential thermogravimetry (DTG), and differential thermal analysis (DTA). In all cases α-Al_2O_3 was used as a blank and analyses took place at a heating rate of 5°C min^{-1} between 20 and 800°C under an air flow of 40 cc min^{-1}. The amount of the sample used in experiment was 100 mg.

3. Results and discussion

The TG/DTG results obtained during heating of the AN containing precursors are shown in Fig. 1.

From this figure it can be seen that in all cases the weight loss takes place at ≈300°C. That means that the products of decomposition of AN, which can proceed according to one or some of the following reactions,

$$NH_4NO_3 \rightarrow NH_3 + HNO_3 \qquad \Delta H = +176\ kJ\ mol^{-1} \quad (1)$$

$$NH_4NO_3 \rightarrow N_2O + 2H_2O \qquad \Delta H = -38\ kJ\ mol^{-1} \quad (2)$$

$$NH_4NO_3 \rightarrow N_2 + 2H_2O + \tfrac{1}{2}O_2 \qquad \Delta H = -120\ kJ\ mol^{-1} \quad (3)$$

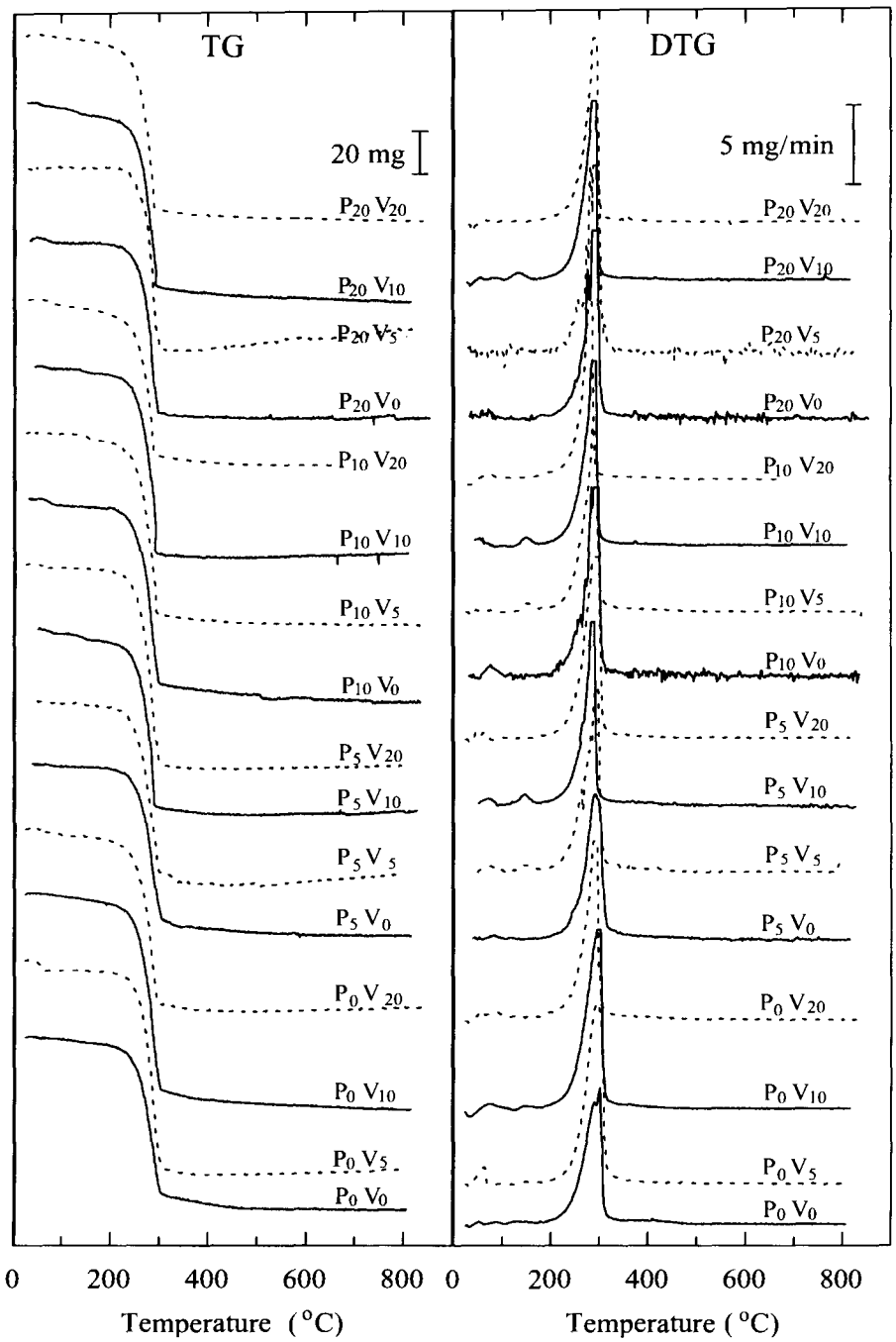

Fig. 1. TG/DTG curves for the $Al_{100}P_XV_Y$–AN solids. The designation for each sample is shown in Table 1.

are removed from the Al–P–V–O containing matrix at about the same temperature leaving back a porous solid.

Nevertheless, although the AN is decomposed at about the same temperature, there is an appreciable differentiation as to the mode of the decomposition which might be exothermal or/and endothermal depending on the sample, as shown in the DTA results in Fig. 2.

In this figure we observe, in all samples, two initial small endothermic peaks, centred around 140 and 180°C and due to the phase transition of AN from Type II to type I structure and to its melting point correspondingly. Following those two peaks there is a large endothermic and/or exothermic signal due to the AN decomposition. In Fig. 3 there is a graphical presentation of the maximum temperature where these DTA peaks, corresponding to the phase transition, the melting point as well as the temperature where the endothermic peak and the exothermic peaks appear.

From this figure we observe that the phase transition of the parent material, without P or V, appears at 138°C as compared to 130°C given in the literature for the pure material. Addition of vanadium seems to inhibit the phase transition by a few degrees to 141–142°C. Subsequent addition of phosphorous (5–10%) decreases the temperature of transition to 137–139°C while further addition (20%) increases it by a few degrees.

As far as the melting point is concerned, it appears at 183°C in the parent material $Al_{100}P_0V_0$–AN as compared to 170°C for the pure NH_3NO_4 compound given in the literature. Addition of phosphorous seems to result in a systematic decrease of it by almost a regular rate of around 0.3 deg/gr-at of phosphorous on the average. In Fig. 3 there is also the variation of the maximum temperature of the exo- and endothermic peak with P and V. The general trend is that of a decrement brought upon both phenomena by the addition of either P or/and V. Fig. 4 also shows the variation of the enthalpy of the exothermic and endothermic peaks as well as their ratio as a function of addition of P and/or V.

From this figure it is apparently clear that the addition of phosphorous as well as vanadium transforms the phenomenon of AN decomposition from a mainly endothermic (reaction 1) to an almost neutral one where the endo- and exothermic routes of AN decomposition are almost matched.

The rate of decomposition can be described by the so-called Coats–Redfern equation

$$\frac{d\alpha}{dt} = k(1-\alpha)^n \tag{4}$$

where α is the percent weight loss at time t, n the reaction order and k the constant usually considered to show an Arrhenius-type dependence on the temperature, $k = A\exp(-E/RT)$. Eq. (4), after integration and taking logarithms becomes

$$\log\left[\frac{1-(1-\alpha)^{1-n}}{T^2(1-n)}\right] = \log\frac{AR}{bE}\left[1-\frac{2RT}{E}\right] - \frac{E}{2.303RT} \tag{5}$$

for $n \neq 1$, whereas, for $n=1$ the left side reduces to $\log[-\log(1-\alpha)/T^2]$, where b is the heating rate given in deg min^{-1}.

Eq. (5) can be plotted in the form of $\log\{[1-(1-\alpha)^{1-n}]/T^2(1-n)\}$ vs. $1000/T$ in order to find the activation energy of the process. It has been shown in Fig. 5 using a computer program, similar to that described by Dhav [7] and applied in similar case previously [8,9], in order to determine the optimum values of n resulting in the best correlation coefficient r.

Fig. 6 shows the obtained apparent activation energies E (kJ/mol), calculated according to this procedure as well as the corresponding order of the reaction n.

It can be seen that the values of E are clustered around 110±20 kJ/mol. No apparent trend appears as a function of P and/or V. The reaction orders n lie in the region 0–0.6 with a clear tendency for higher values at lower addition of P and/or V, which approach zero at 20% addition of P and/or V.

The specific surface areas (ssa, $m^2\,g^{-1}$) of the resulted solids as well as the obtained pore volumes (cc g^{-1}), using the BET procedure, are indicated in Fig. 7 as a function of heteroatoms P and V.

From this figure it is clear that the addition of phosphorous at ~10% levels, at steady addition of vanadium, increases the specific surface as well as the pore volume of the final solids. Addition of vanadium on the other hand, at steady addition of phosphorous,

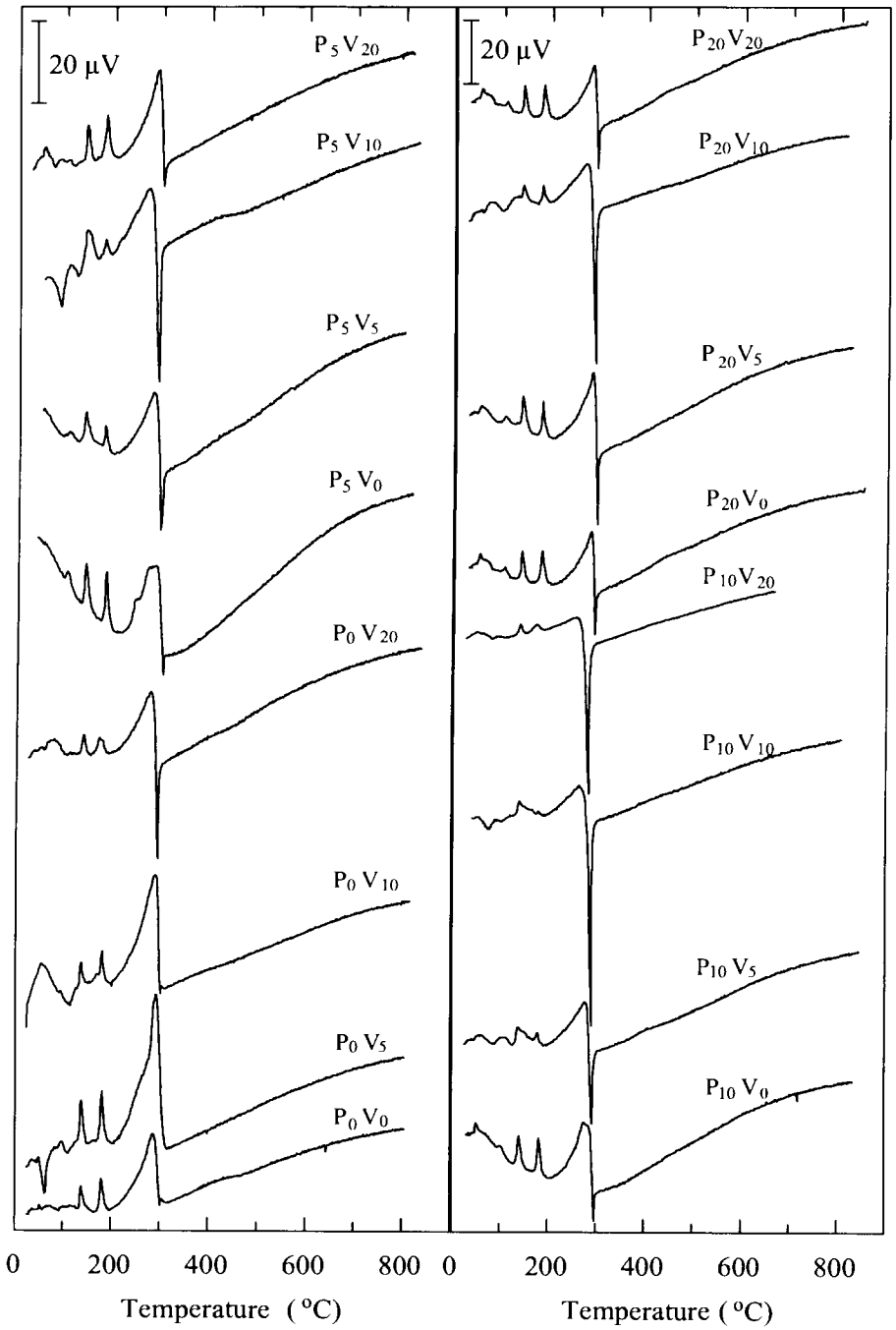

Fig. 2. DTA curves for the $Al_{100}P_XV_Y$–AN solids. Designation similar to Fig. 1.

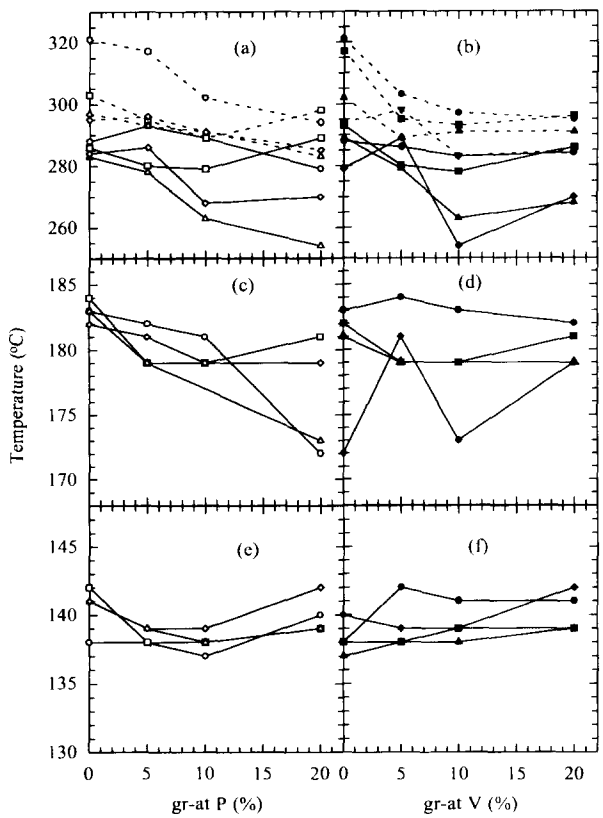

Fig. 3. Variation of maximum temperature of the exo (dashed line) and endo (solid line) effect of NH_4NO_3 decomposition in $Al_{100}P_XV_Y$ matrices (a, b), of the melting point of NH_4NO_3 (c, d) and of the phase transition of NH_4NO_3 (e, f). (○, ●) – 0%, (□, ■) – 5%, (△, ▲) – 10% and (◇, ◆) – 20%, open symbols for vanadium and black for phosphorus.

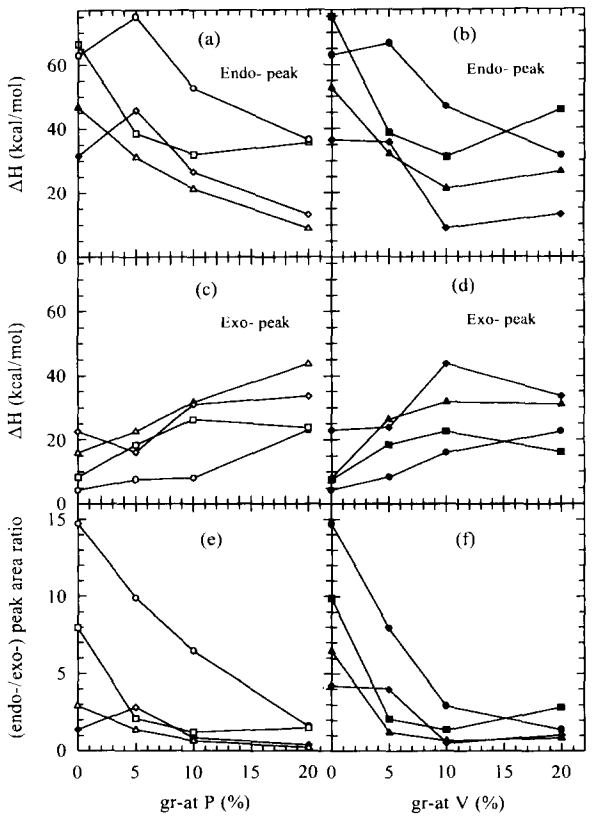

Fig. 4. Enthalpy corresponding to endo- (a, b) and exothermic effects (c, d) of $Al_{100}P_XV_Y$–AN decomposition. The $(-\Delta H)$ values were calculated from the corresponding peak area. (e, f) ratio of endo/exo peaks as a function of P and V content at the solids. (○, ●) – 0%, (□, ■) – 5%, (△, ▲) – 10% and (◇, ◆) – 20%, open symbols for vanadium and black for phosphorus.

increases only the surface area at 5% doping, while its influence on the pore volume is negligible.

The maximum values of the specific surface areas achieved by these materials which approach 350–380 $m^2\ g^{-1}$ as well as the pore volume which is higher than 1 cc g^{-1} make such solids promising for adsorption studies. The phenomenon of synergy between P and V in influencing both the external area and the voids created is remarkable. This synergistic action of the two pentavalent elements P and V is not well understood up to now. A suggestion made is that phosphorous creates a two-dimensional oligophosphate net on the surface of alumina, protecting it from collapsing to bulkier structures [5,6]. Similar action of phosphorous protecting the stability of other high surface area mesoporous materials has been recently observed [10]. In the past, the development of the surface area of similar solids has been indeed related to the mode of the thermal decomposition of precursors [11]. The action of vanadium might be explained along similar lines, in other words creation of oligomeric species which stay on the external surface and acting protectively as to the sintering of the solids. Nevertheless, the action of vanadium itself is less profound as compared to that of phosphorous. It may be possible that oligo-polymeric phosphoro–vanadates species created at certain ratio P/V on the surface of alumina substrate are of increased thermal stability and thus protect the structure from collapsing

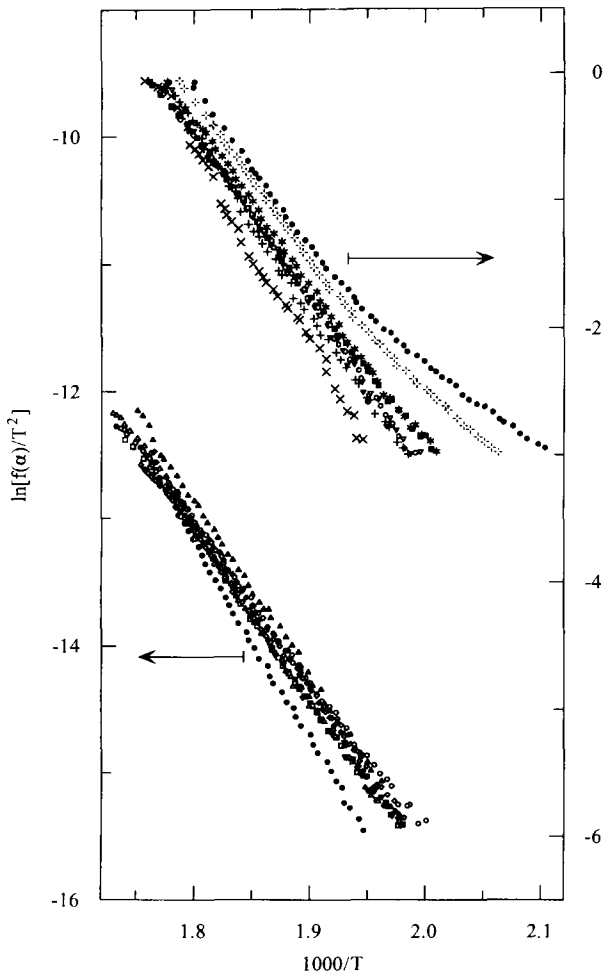

Fig. 5. Arrhenius plots for the calculation of activation energy E_a of decomposition according to the Coats–Redfern procedure.

under thermal shock. Although a clear correlation is not apparent at first glance between the examined thermal decomposition characteristics and the final surface properties of the solids, there is a tendency for the materials with ratio of exo/endo effect about unity to produce materials with higher surface areas. This is shown in Fig. 8 where the log of the ratio endo/exo peak areas have been plotted versus the corresponding specific surface areas.

Although some points are out of trend, the general picture is unmistakable: The development of high surface areas in the examined Al–P–V solids is more often the result of 'balanced' or almost 'neutral' total

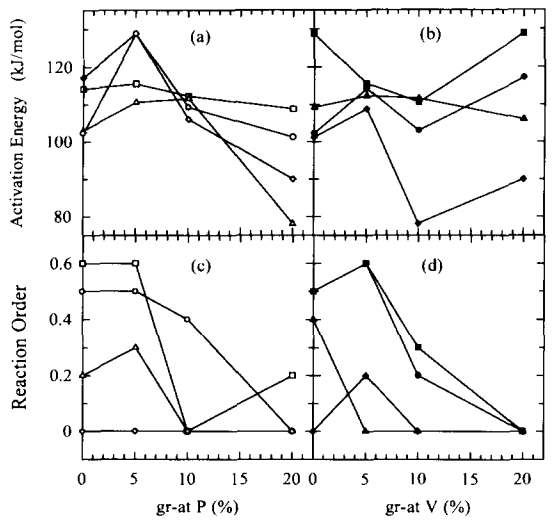

Fig. 6. Activation energies (a, b) and reaction order (c, d) for the $Al_{100}P_XV_Y$–AN decomposition as a function of P and V in the solids. (○, ●) – 0%, (□, ■) – 5%, (△, ▲) –10% and (◇, ◆) – 20%, open symbols for vanadium and black for phosphorus.

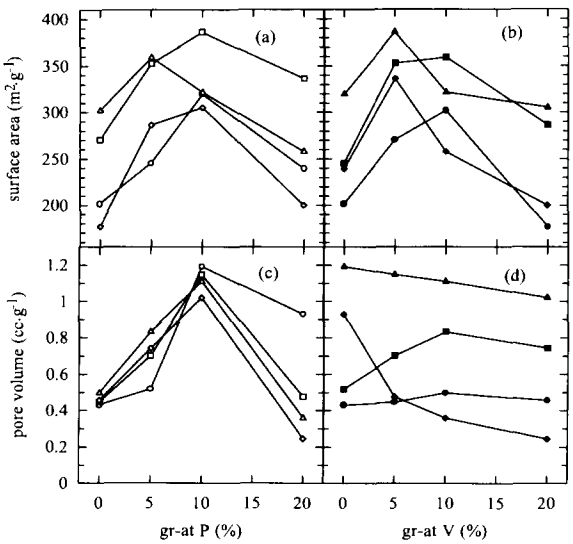

Fig. 7. Variation of the specific surface area (a, b) and the pore volume (c, d) of the fired (600°C) $Al_{100}P_XV_Y$ solids. (○, ●) – 0%, (□, ■) – 5%, (△, ▲) – 10% and (◇, ◆) – 20%, open symbols for vanadium and black for phosphorus.

thermo-effect of the NH_4NO_3 precursor decomposition. Actually a similar effect has been already observed in a previous work [11]. It is observed that

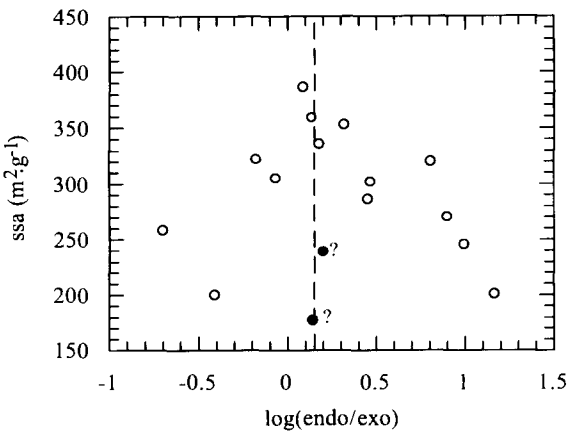

Fig. 8. Variation of the specific surface area of the fired (600°C) $Al_{100}P_XV_Y$ solids as a function of the log of the ratio endo/exo peak areas. All samples are included.

the maximum in the ssa in Fig. 8 appears at log(endo-/exo-)≈0.15 which means that the ratio of endo- to exo-effect is around 1.41. This is a remarkable result since this ratio almost matches the ratio of enthalpies of endothermic decomposition of NH_4NO_3 (see reaction 1) to that of its exothermic decomposition (reaction 3) which is 176/120=1.466. In other words, when the endothermic and exothermic routes are almost balanced and the total effect is thermally neutral, then the material develops the highest internal surface. Such observations are in line with the well-known practice that the development of high surface area solids is a result of careful drying under high temperature condition or drying under low pressure at low temperature (lyofilization). It seems that thermochemical studies like the present one and the one mentioned in Ref. [11] provide the experimental background for the middle-way-heating practices applied by the workers in the field of porous materials.

Acknowledgements

This work was supported by PENED-95 program.

References

[1] J. Haggin, Chem. Eng. News, 1, Oct. 1990, 2.
[2] M.J. Hudson and C.A.C. Sequeira (Eds.), Multifunctional Mesoporous Materials, NATO ASI Series C: Vol 400 Kluwer Academic Publishers, Durdrecht, Boston, London (1993).
[3] J.S. Beck, J.C. Vartuli, W.J. Both, M.E. Leonowicz, C.T. Kresge, K.D. Shmidt, C.T.-W. Chu, D.H Olson, E.W. Sheppard, S.b. McCullen, J.B. Higgins and J.L. Schlenker, J. Am. Chem. Soc., 114 (1992) 10834.
[4] A. Monnier, F. Schüth, Q. Huo, D. Kumar, D. Margolese, R.S. Maxwell, G.D. Stuky, M. Krishnamurty, P. Petroff, A. Firouzi, M. Janicke and B.F. Chmelka, Science, 261 (1993) 1299.
[5] D.E. Petrakis, M.J. Hudson, A.T. Sdoukos, P.J. Pomonis and T.V. Bakas, Colloids and Surfaces A: Physicochemical and Engineering Aspects, 90 (1994) 191.
[6] D.E. Petrakis, M.J. Hudson, A.T. Sdoukos, P.J. Pomonis and T.V. Bakas, J. Mater. Chem., 5(11) (1995) 1975.
[7] R.S. Dhav, Computer and Chemistry, 10 (1986) 293.
[8] S. Skaribas, T.C. Vaimakis and P.J. Pomonis, Thermochimica Acta, 158 (1990) 235.
[9] T.C. Vaimakis, P.J. Pomonis and A.T. Sdoukos, Thermochimica Acta, 173 (1990) 101.
[10] U. Cielsa, S. Schacht, G.D. Stuky, K.K. Unger, F. Schüth, Angew. Chem., 108 (1996) 597; Angew. Chem. Int. Ed. Engl., 35 (1996) 541.
[11] C.S. Skordilis and P.J. Pomonis, Thermochimica Acta, 216 (1993) 137.